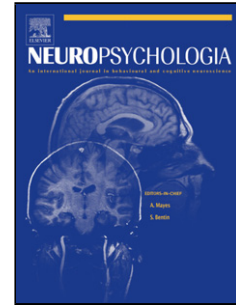# Accepted Manuscript

Title: A big-world network in ASD: Dynamical connectivity analysis reflects a deficit in long-range connections and an excess of short-range connections.

Authors: Pablo Barttfeld, Bruno Wicker, Sebastián Cukier, Silvana Navarta, Sergio Lew, Mariano Sigman

Please cite this article as: Barttfeld, P., Wicker, B., Cukier, S., Navarta, S., Lew, S., & Sigman, M., A big-world network in ASD: Dynamical connectivity analysis reflects a deficit in long-range connections and an excess of short-range connections., *Neuropsychologia* (2010), doi:10.1016/j.neuropsychologia.2010.11.024

A big-world network in ASD: Dynamical connectivity analysis reflects a deficit in long-range connections and an excess of short-range connections.

Pablo Barttfeld[1,2], Bruno Wicker [1,3], Sebastián Cukier[1,2], Silvana Navarta[1] , Sergio Lew[4] and Mariano Sigman[1]

[1]Integrative Neuroscience Laboratory, Physics Department, University of Buenos Aires.
[2]Fundación para la Lucha contra las Enfermedades Neurológicas de la Infancia, Buenos Aires.
[3]Mediterranean Institute of Cognitive Neurosciences, Centre National de la Recherche Scientifique, Université de la Méditerranée, 31 Chemin Joseph Aiguier, 13402 Marseille Cedex 20, France.
[4]Instituto de Ingeniería Biomédica, Facultad de Ingeniería, Universidad of Buenos Aires

Corresponding author: Pablo Barttfeld
Integrative Neuroscience Laboratory, Physics Department, University of Buenos Aires, Buenos Aires, Argentina.
e-mail:pbarttfeld@fi.uba.ar

Abstract

Over the last years, increasing evidence has fuelled the hypothesis that Autism Spectrum Disorder (ASD) is a condition of altered brain functional connectivity. The great majority of these empirical studies relies on functional magnetic resonance imaging (fMRI) which has a relatively poor temporal resolution. Only a handful of studies has examined networks emerging from dynamic coherence at the millisecond resolution and there are no investigations of coherence at the lowest frequencies in the power spectrum –which has recently been shown to reflect long-range cortico-cortical connections. Here we used electroencephalography (EEG) to assess dynamic brain connectivity in ASD focusing in the low-frequency (delta) range. We found that connectivity patterns were distinct in ASD and control populations and reflected a double dissociation: ASD subjects lacked long-range connections, with a most prominent deficit in fronto-occipital connections. Conversely, individuals with ASD showed increased short-range connections in lateral-frontal electrodes. This effect between categories showed a consistent parametric dependency: as ASD severity increased, short-range coherence was more pronounced and long-range coherence decreased. Theoretical arguments have been proposed arguing that distinct patterns of connectivity may result in networks with different efficiency in transmission of information. We show that the networks in ASD subjects have less Clustering coefficient, greater Characteristic Path Length than controls -indicating that the topology of the network departs from small-world behaviour- and greater modularity. Together these results show that delta-band coherence reveal qualitative and quantitative aspects associated with ASD pathology.

Running title: Functional EEG connectivity in Autism.

2

1. Introduction

Autism or Autism Spectrum Disorder (ASD) is a neurodevelopmental disorder characterized by a triad of impairments in social interaction, communication, and behavioural flexibility (APA, 2000). There is increasing evidence that ASD could be a condition of altered brain connectivity (Belmonte et al., 2004; Courchesne & Pierce, 2005; Just, Cherkassky, Keller, Kana, & Minshew, 2007; Just, Cherkassky, Keller, & Minshew, 2004; Markram, Rinaldi, & Markram, 2007; Wicker, 2008). Anatomical studies showed that individuals with ASD have smaller and more densely packed columns of neuronal cells (Casanova & Trippe, 2009; Casanova, Switala, van Engeland, Heinsen, Steinbusch, Hof, Trippe, Stone, Schmitz, 2006; Hughes, 2007). Structural MRI studies have reported a reduced corpus callosum (Alexander et al., 2007; Egaas, Courchesne, & Saitoh, 1995) and abnormal anatomy and connections of the limbic–striatal social brain system in ASD (McAlonan et al., 2005). fMRI studies also yielded evidence of altered connectivity: connectivity within the frontal lobe seems differently organized, and areas such as prefrontal cortex, precuneus/posterior cingulate cortex and superior temporal sulcus, appear to be poorly connected (Just, Cherkassky, Keller, Kana, & Minshew, 2007; Just, Cherkassky, Keller, & Minshew, 2004; Kleinhans et al., 2008; Koshino et al., 2005; Mason, Williams, Kana, Minshew, & Just, 2008; Welchew et al., 2005). Recent fMRI studies have moved away from the social and cognitive deficit models and looked at the functional connectivity between areas of the so-called default mode network (DMN), i.e. networks that become activated at rest (Gusnard & Raichle, 2001; Raichle, 2009). Results revealed decreased connectivity between the medial prefrontal cortex and precuneus/posterior cingulate cortex (Cherkassky, 2006; Di Martino et al., 2009; Weng, 2010). The great majority of the evidence signalling functional connectivity as a key aspect of ASD was obtained using fMRI. There is only a handful of studies assessing ASD brain connectivity using the other canonical tool to study connectivity, electroencephalography (EEG). Abnormal gamma activity has been reported in autistic children, interpreted as supporting hypotheses of abnormal connectivity (Brown, Gruber, Boucher, Rippon, & Brock, 2005). (Murias, 2008) and (Coben, Clarke, Hudspeth, & Barry, 2008) measured connectivity more directly using EEG coherence and reported evidence of both under and over-connectivity in different frequency bands in ASD populations. Understanding the patterns of connectivity in low frequencies -the delta band- remains unexplored.

3

Over the last years, analysis of coherence at low-frequencies has gained great interest. Long-range intra-cortical and feedback cortico-cortical connections, which are thought to be altered in ASD, are revealed by the slow cortical potentials (SCP) of the EEG (He & Raichle, 2009; He, Zempel, Snyder, & Raichle, 2010). Information of the rectified power of the SCP, although distinct and dissociable from the raw signal e.g., during vigilance tasks (He, Zempel, Snyder, & Raichle, 2010) also correlates with the resting-state fMRI signal (Lu, 2007).

We investigated whether functional brain networks in EEG are abnormally organized in the delta band in ASD, measuring coherence in the raw filtered signals (He & Raichle, 2009; He, Zempel, Snyder, & Raichle, 2010). We will show that control subjects have stronger long fronto-occipital connections, and weaker lateral frontal connections and, moreover, that these differences are good predictors of ASD severity. When inspecting the impact of this connectivity pattern on the global organization of functional network using graph theory measures we observed that ASD present higher Characteristic Path Length (L), smaller Clustering Coefficient (C) and higher modularity index (MI), resulting in a less efficient brain network (Latora & Marchiori, 2001).

2. Material and Methods.

2.1 Participants

Two groups took part in this study. The ASD group included 10 adults with high-functioning autism or Asperger's syndrome (9 men and 1 women; mean age = 23.8, std = 7.6, Table 1). The individuals with ASD were provisionally accepted into the study if they had received a diagnosis of infantile autism or Asperger's syndrome from a child psychiatrist, developmental pediatrician, or licensed clinical psychologist. Actual participation required that this diagnosis had been recently confirmed, with each subject having met the criteria for ASD within the past 3 years on the basis of the revised fourth edition of the Diagnostic and Statistical Manual of Mental Condition (APA, 2000) and on the score on the Autistic Diagnostic Observation Schedule-Generic (Lord et al., 2000). The IQs were measured with the third edition of the Wechsler Adult Intelligence Scale and ranged from 85 to 125 (mean=101.7, SD=14.97). At the time of testing, no ASD subject had known associated medical condition. As their mean IQ

4

score was within the normal range, the ASD participants were individually matched to a group of 10 typically developing individuals on the basis of sex and chronological age.

The participants in the control group (9 men, 1 women, mean age = 25.3, std = 6.54). None of the volunteers had reported history of neurological or psychiatric conditions.

2.2 EEG recordings.

EEG were recorded with a Biosemi ActiveTwo 128 channel 24-bit resolution system, with active electrodes (first amplifying stage on the electrode to improve signal to noise ratio), digitalized at 512 Hz and low-passed DC-1/5th of the sample rate (-3dB) by a 5th order digital sync anti-aliasing filter. There were no additional hardware filters during acquisition. 7-minute temporal signals were recorded during an eyes-closed resting while subjects sat on a reclining chair in a sound attenuated room with a dim light. During the experiment, particpants and EEG recordings were monitored to assure that they mantained vigilance and did not fall asleep. After the acquisition, signals were re-referenced to the average of all electrodes, and filtered on the delta band (0.5-3.5 Hz, ~60dB/decade roll-off). The signal was filtered using the function eegfilt.m from the EEGLAB toolbox (Delorme & Makeig, 2004). This function implements a two-way least squares finite impulse response filter. Filter order was calculated as

$$\frac{3.SamplingRate}{Low\_Cuttoff} = 3072$$

Synchronisation between all pair wise combinations of EEG channels were computed for all subjects with the Synchronisation Likelihood (SL) method (Montez, Linkenkaer-Hansen, van Dijk, & Stam, 2006). All the details of the methodology can be found at (Montez, Linkenkaer-Hansen, van Dijk, & Stam, 2006). For clarity here we outline the critical aspects of the method.

The SL method maps the original data to a set of vectors, essentially resampling the data at variable time bins (Lags), referred as embedding vectors. An embedding vector has the form:

$$X_{k,i} = (X_{k,i}, X_{k,i+L}, X_{k,i+2L}, X_{k,i(m-1)L})$$

5

Where k is the channel number, i is a sample reference of the raw data, L is the lag and m is the length of the vector, which will determine the dimension of the state space to search for similarity. In our analysis L and m were set to 49 and 22. These values, as all the parameters, were set following (Montez, Linkenkaer-Hansen, van Dijk, & Stam, 2006). The embedding vectors are then used to localize times series with recurrent dynamical themes for each electrode. This is done by measuring the Euclidean distance among a fixed reference vector $X_{k,i}$ and the set of all embedded vectors $X_{k,j}$ that lie in a window around time i (this window was fixed to 3049). From this analysis, for each electrode and each value of i, one obtains the set of similar vectors (or "recurrences"), arbitrarily defined as the 5% of vectors closest to $X_{k,i}$. Then, for each time i we compute SL between channels *k1* and *k2* measuring the similitude between their closest reference vectors (i.e. the distributions of recurrences).

$$SL_i = \frac{n_{k1k2}}{n_{k1}}$$

where n_{k1k2} is the number of coincident recurrences found in channel *k1* and in channel *k2* at time i and n_{k1} is the number of recurrences found in channel *k1* at time i. A SL value close to 1 means that all recurrences of channel *k1* are shared and coincident with the recurrences of channel *k2*. Repeating the procedure for all i (i.e. sliding the method in time) we obtained a time series of SL for each pair of channels.

This procedure was conducted independently for each participant in the study. Hence, from this analysis we obtained from each participant a matrix of 128x128xNsamples. We then collapsed this 3 dimensional matrix into a symmetrical matrix, where each entry in the matrix represents the SL between the corresponding pair of electrodes averaged throughout all samples. All subsequent analysis and statistics were performed on these SL matrices.

2.3 Graph Theory metrics.

The connectivity matrix defines a weighted graph where each electrode corresponds to a node and the weight of each link is determined by the SL of the electrode pair. To calculate network measures, SL matrices were converted to binary undirected matrices by applying a threshold *T*. We explored a broad range of values of $0.01 < T < 0.2$, with increments of 0.0005 and repeated the full analysis for each value of *T*. After

6

transforming the SL-matrix to a binary undirected graph, we measured the Clustering Coefficient *C*, the Characteristic Path Length *L* and Modularity Index *MI* using the BCT toolbox (Rubinov & Sporns, 2009). For statistical comparisons of graph based metrics, we performed ANOVAs with group (control or ASD) and threshold (binned in 8) as independent factors. Errors were calculated using bootstrap (Efron & Tibshirani, 1994), which were used to explore statistical differences for all individual thresholds. The bootstrap probability was also calculated, resampling 2000 times each metric for both groups, and calculating the percentage of times the mean metric of a group was larger than the mean metric of the other group. Network visualizations were performed using the Pajek software package (Batagelj & Mrvar, 1998) using a Kamada-Kawai layout algorithm (Kamada & Kawai, 1989).

3. Results

For each participant in this study, we calculated the Synchronization Likelihood (SL) across all pairs of channels -see methods and (Montez, Linkenkaer-Hansen, van Dijk, & Stam, 2006) for details. SL provides a measure of temporal coherence between two temporal signals. This measure is more sensitive than simply a linear-correlation because: 1) it does not assume linearity in the coherence and 2) it is sensitive to phase-shifted coherent frequency bands which may result in a null linear correlation. This analysis collapsed the stationary EEG data of each participant, band passed in the delta range to a 128x128 synchronization matrix (henceforth referred as SL-matrix). The element *(i,j)* of the matrix provides a measure of the temporal similarity at low frequencies of electrodes *i* and *j* during eyes-closed stationary EEG, which we refer as functional connectivity. In what follows, we analyse statistical differences in functional connectivity for ASD and control population.

To calculate significant differences in SL patterns across groups, we conducted a paired t-test with the SL value for each pair of channels (Figure 1b). A positive t-value indicates that SL increased in control compared to ASD population. Conversely, a negative t-value indicates that SL is greater in ASD than in the control population. The distribution of t-values (Figure 1d) was significantly shifted towards positive values (mean= 0.57; std= 1,11; t-test: p=0, CImin= 0.55; CImax=0.58) indicating that the global trend was that SL was greater in the control population. Our interest was to understand the topography of the tails of this distribution, i.e. which pairs of electrodes

7

had a greater difference in SL between ASD and control population. For this, we simply determined an arbitrary cut-off at t = 2 (Figures 1b and 1d) and considered the resulting matrix with values 1, 0 or -1 depending on whether t > 2, 2>t > -2 or -2 > t (Figure 1f). This cut-off is certainly arbitrary but none of the results discussed in what follows depend on this choice (see Supplementary Figure 1 for a progression of the synchronization topographies for varying thresholds). The previous mask filters pairs of electrodes for which we found significant differences in similarity between both groups. To further constrain the number of comparisons and generate a relatively sparse pattern of connections amenable to visualize its topography, we considered only pairs of electrode with sufficient similarity for both groups. This was achieved applying a mask resulting from the intersection of pairs of electrodes with SL > 0.03 for the patients and for the controls grand average (Figures 1c and 1e).

The topographic projections of connections whose strength increased (red) or decreased (blue) in ASD compared to control participants (Figure 1h) showed a very consistent pattern. Connections which were stronger in the control group were localized in the frontal lobe and extended over the midline to the occipital cortex. They also included long-range connections between these regions. On the contrary, connections which were stronger in the ASD group were very focal and largely localized to the lateral frontal electrodes. These observations did not change qualitatively when changing the thresholds of the binary difference matrix or the activation mask (Supplementary Figure 1).

To further quantify these observations, and to explore in a statistical manner whether fronto-occipital interactions are greater in control group and lateral-frontal interactions in the ASD group, we defined four different regions: Mid Frontal, Frontal Right, Frontal Left and Occipital (Figure 2a). We then measured global connectivity across regions (including the connectivity of a region with itself), performing a t-test comparing the SL value of the weighted SL-matrix for all pairs of electrodes of the corresponding regions. This analysis revealed that local connections in Mid Frontal decrease in ASD compared to controls (t-test: $t(1,9)=3.02$; p=0.01), as well as the long connections between Mid Frontal and Occipital (t-test: $t(1,9)=2.21$; p=0.05) (Figure 2b). On the contrary, local connections in both Lateral Frontal areas are enhanced in ASD, being significant only in the Frontal Left (t-test: $t(1,9)=-2.35$; p<0.05), not in the Frontal Right (t-test: $t(1,9)=-$

8

0.82; p>0.1). All other combinations of regions (Figure 2b) showed no statistical diferences.

The previous analysis showed consistent and topographically organized differences in SL between ASD and control groups, suggesting that a distinct pattern of dynamical connectivity may be related to the physiopathology of ASD. A more severe test to this hypothesis involves examining progressive changes in connectivity with a continuous progression of ASD. To examine whether the observed difference in connectivity progressed with ASD severity, we measured the correlations between ADOS score – which indexes ASD severity and varied from 7 to 16 within our population- and SL-connectivity of each pair of electrodes. Figure 3a shows two representative examples of SL pairs with a negative (blue) and a positive (red) correlation with ADOS score. The topographical distribution of the correlation of ADOS within the ASD population followed the same pattern than SL differences between groups: medial electrodes are negatively correlated with ADOS (and hence their SL is greater with decreasing levels of ASD and progressing to control population); on the contrary lateral electrodes, predominantly short local connections, have SL values which increase with ADOS score. Note that, also coherently with the group analysis, the global trend is that negative correlations (blue edges, Figure 3b) are more prominent indicating that, on average, SL connectivity decreases with increasing level of ASD. To test quantitatively the hypothesis that short-range connections are overweighed in ASD and long-range connections are scanter, we measured the distribution of correlation coefficients for all pairs of electrodes at any given length[1] (Figure 3c). Positive correlations (SL increases with ADOS score) were very significant only within a very short range. On the contrary negative correlations (SL increases with decreasing ADOS score) were broadly distributed and extended over distant pairs of electrodes (Figure 3c). This scaling effect becomes clearer in a more quantitative manner when considering the mean value of positive and negative correlations averaged across all pairs at a fixed distance (Figure 3d). These results confirm our findings based on group analysis: ASD connectivity is overall of shorter range and dominantly localized to lateral region of the brain, with a deficit of medial occipito-frontal connections.

---

[1] Here we considered the planar distance between pairs of electrodes. This is only an approximation as interactions reflect coherent sources in a 3D volume. For the purpose of this analysis, were we merely want to explore broad scaling properties, this approximation seems adequate. Analyzing distributions considering spherical distances yielded virtually the same result.

9

The previous analysis shows that ADOS is a good predictor of the precise pattern of SL connectivity. The IQ distribution of patients was in the normal range, but patients were not matched individually to controls (i.e. there was not a one to one correspondence of IQ between both groups). To assure that the effect of ADOS in SL pattern of connectivity was not biased by correlations with IQ we measured the correlations between ADOS and IQ in the patient group. ADOS and SL were largely independent (Figure 4a, linear regression between both variables, $p > 0.45$). While this shows that the effect of ADOS on SL is unlikely to be accounted by covariations with IQ, IQ still may explain residual variance of SL patterns. To investigate a possible effect of IQ in SL we performed a multiple regression of SL (one for each pair of channels, as done above), with IQ and ADOS as regressors. The effect of ADOS is virtually identical to the previous analysis, which is expected if both variables are independent (compare figure 3b and figure 4d). A direct comparison of correlation matrices for IQ and ADOS (Figure 4b and 4c) shows that IQ covariations are very weak, implying that it has virtually no effect on our observables.

We next investigated whether these differences resulted in network topologies which may have consequences in properties of information flow in the ASD and control group. Using the Kamada Kawai algorithm (Kamada & Kawai, 1989), we embedded the ASD and control networks, showing the 1000 strongest connections, in the two-dimensional plane (Figure 5a; visualizations of the networks at fixed threshold gave qualitatively the same results, see Supplementary Figure 2). By simple inspection, it is evident that the networks are qualitatively different. Control network presents a central core of nodes – composed mainly by Mid-Frontal and Occipital electrodes, considering the regions defined in Figure 2a. The ASD network is homogeneously connected, has a larger diameter and appears to be more modular and less clustered.

To quantify these observations we used four canonical graph theory metrics: Degree (K), Characteristic Path Length (L), Clustering Coefficient (C) and Modularity Index (MI). The degree (K) of the network, which constitutes its simplest statistical indicator, simply measures the average number of neighbours of each node (Figures 5b and 5c). As expected, K diminished as the threshold increases, disconnecting nodes and diminishing the size of the network (Stam, Jones, Nolte, Breakspear, & Scheltens, 2007). To investigate the effect of ASD on K, we submitted the K values to an ANOVA

10

with group (control or ASD) and T (binned in 8) as independent factors. Results revealed a significant effect of group (F(1,1)=14.48; p<0,01) as well as for threshold (F(1,7)=662; p<0,01), and a significant interaction between both factors (F(1,1)=12.15; p<0,01). This shows that K was higher for the control group and that this effect is not invariant for all thresholds (Figure 5b). To further quantify where the differences between groups are located, we conducted a bootstrap analysis to compare K at every threshold. We found that for an intermediate range of T values (0.034-0.093), the degree was significantly higher in controls than in ASD, the most significant difference found for T = 0.056 (bootstrap test, P<0.01). At this threshold, we explored the topography of K for both groups. The scalp in Figure 5c shows the difference between scalps of both groups (Control – ASD). As with our previous findings, while the main finding is that K increases for controls compared to ASD *on average*, it displays a rich topographical distribution with areas showing larger K and areas showing smaller K than ASD: Control group shows larger K than ASD in the Mid Frontal and Occipital areas, and smaller K in the lateral fronto-parietal regions, a distribution consistent with the observed pattern in figures 1 and 2 (green dots mark electrodes where $K_{control} > K_{ASD,}$; pink dots mark electrodes where $K_{ASD} > K_{control}$, p<0.01).

To quantify the notion of homogeneity we measured the distribution of K at different nodes (simply comparing the max and min K, a standard deviation of the distribution yielded the same results). Variations in K were less pronounced in ASD networks. At a fixed threshold the relation min(K) / max(K) for a given subject is larger in ASD than in Controls (mean controls = 0.02; mean ASD = 0.05; t(1,9): 2.39; p<0.05) demonstrating a more homogeneously connected network in ASD.

The overall dependence of the Characteristic Path Length with T also followed a well known behaviour (Figure 5d). As T increases, less edges remain and hence L increases. For very high values of T, the graph disconnects in several components, only short-range links remaining and hence L starts decreasing. To investigate the effect of ASD on Characteristic Path Length, we submitted L to an ANOVA with group (control or ASD) and T (binned in 8) as independent factors. Results revealed a significant effect of group (F(1,1)=8.56; p<0,05) as well as for threshold (F(1,7)=186; p<0,01), and a significant interaction between both factors (F(1,1)=4.91; p<0,01), showing that L was higher for the ASD group (Figure 5d). To further quantify at which thresholds differences between groups were significant, we conducted a bootstrap analysis to

11

compare L at every threshold. At an intermediate range of values of *T* (0.042-0.073), L is significantly larger for the ASD group, the most significant difference found at T = 0.056 (bootstrap test, p< 0.01).

We performed the same analysis to examine whether Clustering coefficient of ASD and Control networks differed (Figure 5e). We submitted C to an ANOVA with group (control or ASD) and T (binned in 8). Results revealed a significant effect of group $(F(1,1)=120.23;\ p<0,01)$ as well as for threshold $(F(1,7)=295;\ p<0,01)$, and a non significant interaction between both factors $(F(1,1)=1.88;\ p>0.05)$, showing that the C was higher for the control group (Figure 5e). Post-hoc bootstrap analysis comparing C at every threshold showed that, at an intermediate range of values of *T* (0.017-0.044), C is significantly larger for the control group; the most significant difference is found for T = 0.032 (bootstrap test, p < 0.01).

Much effort has been devoted to the study of statistical indicators of networks, particularly the Characteristic Path Length and the Clustering Coefficient. An ubiquitous present topological network usually referred to as small-world, which has a relatively short (compared to random networks) Characteristic Path Length and high Clustering Coefficient has been shown to be optimal for information transfer and storage (Sporns & Zwi, 2004). Our combined findings (increased L and decreased C in ASD compared to control networks) indicate that the ASD network topology is consistently farther from being a small world than control network.

A direct consequence of the lack of long-range connections found in ASD is that cortical areas may become relatively isolated from each other, resulting in turn in a more modular organization (Galvao et al., 2010; Gallos, Song, Havlin, & Makse, 2007). To assess this in a quantitative manner, we estimated the Modulation Index (MI) that estimates the tendency of a network to split into modules. The dependence of MI with T follows a similar trend than L (Figure 5f): as T increases, less edges remain and MI (and the number of actual modules) increases. To investigate the effect of ASD on MI, we submitted this data to an ANOVA with group (control or ASD) and T (binned in 8) as independent factors. Results revealed a significant effect of group $(F(1,1)=40.76;\ p<0,01)$ as well as for threshold $(F(1,7)=220;\ p<0,01)$, and a significant interaction between both factors $(F(1,1)=18.64;\ p<0,01)$, showing that the MI was higher for the ASD group (Figure 5f). To further quantify where the differences between groups are

12

located, we conducted a bootstrap analysis to compare MI at every threshold. We found that for a very wide range of values of T (0.005-0.14), MI is significantly larger for the ASD group, the most significant difference found at T = 0.065 (bootstrap test, P < 0.01)

4. Discussion

The main purpose of this study was to characterize and compare resting state functional brain networks in subjects with ASD and neurotypical subjects. We studied networks derived from stationary EEG data filtered in the delta band. We observed reliable and consistent differences in the connectivity patterns of both groups. ASD subjects showed a lack of long-range, fronto-frontal and fronto occipital connections, and an enhancement of local, lateral frontal connections. While the spatial resolution of EEG is limited, the topographical analysis reported here can only be understood as referring to broad cortical regions. With this caveat and note of caution, our results are consistent with fMRI data showing diminished or lack of connectivity in the midline, more specifically between the medial prefrontal cortex and precuneus (Courchesne & Pierce, 2005; Hughes, 2007; Kana, 2006; Weng, 2010). Similarly, our observation of increased connectivity in prefronto-lateral nodes might be related with a lack of inhibition in dorsolateral Prefrontal cortex or altered connectivity of the Anterior Insula, (Di Martino et al., 2009; Kennedy, Redcay, & Courchesne, 2006; Weng, 2010).

Beyond broad group differences, our observation of a coherent topographic representation in a parametric measure of ASD determined by the ADOS score is indicative of a gradual change of network properties with increasing severity of the syndrome. Our results also revealed global trends related to proximity of correlations and ASD: for increased ASD severity, local connections increased monotonically and long range connections decreased. This global trend is also inline with fMRI results relating the severity of ASD and fMRI correlation (Di Martino et al., 2009; Kennedy, Redcay, & Courchesne, 2006; Weng, 2010).

Changes in connectivity patterns have an impact in the global organization of a network which in turn determine the efficiency of information transfer and storage (Barabasi, 2009; Galvao et al., 2010; Gallos, Song, Havlin, & Makse, 2007; Sigman & Cecchi, 2002; Sporns & Zwi, 2004). Small-world networks have attracted great attention during the last decade (Watts & Strogatz, 1998) because they are ubiquitously present in a

13

broad range of natural phenomenon but also because they establish an optimal balance between local specialization and global integration (Sporns & Zwi, 2004). We tentatively suggest that the functional networks of ASD subjects reveal a big-world structure, which may depart from an optimal organization for information processing and storage.

Cortico-cortical connections can be roughly classified in two main groups (Schroeder & Lakatos, 2009; Sporns & Zwi, 2004): local connections linking neurons in the same cortical area (critical in generating functional specificity i.e., information) and long-distance connections between neurons of different cortical regions, that ensure that distant cortical sites can interact rapidly to generate dynamical patterns of temporal correlations, allowing the integration of different sources of information into coherent behavioural and cognitive states (Bressler, 1995; Friston, 2002; Nicoll, Larkman, & Blakemore, 1993; Sporns & Zwi, 2004). The differences we found in this study suggest that this compromise is unbalanced in ASD. The reduced long range connections may provide a physiological measure for the lack of proper integration of information observed in ASD (Frith, 1989). In this sense, the organization of the whole brain networks might be related with the known differences in information processing between typical and ASD individuals.

A ubiquitous aspect of brain function is its modular organization, with a large number of processors (neurons, columns or entire areas) working in parallel. The workspace theory argues that a distributed set of neurons with long axons provides a transient global "broadcasting" system enabling communication between arbitrary and otherwise not directly connected brain processors (Baars, 1988; Baars, 2005; Dehaene & Naccache, 2001). While at this stage merely speculative and requiring further investigation, these findings suggest that ASD individuals may have an atypical workspace system, revealed in enhanced local connectivity, a more homogeneous network lacking hubs and central nodes, and a more modular organization. While the workspace system conveys brain function with a flexible communication protocol this comes at a cost: it is slow and intrinsically serial (Pashler & O'Brien, 1993; Sergent, Baillet, & Dehaene, 2005; Sigman & Dehaene, 2008; Zylberberg, Fernandez Slezak, Roelfsema, Dehaene, & Sigman). Hence, a functional manifestation of the ASD network might be to favour more parallel processing of information –being the cost of

14

this enhancement the lack of behavioural flexibility, core symptom of individuals with ASD- an idea that resonates with the well known skills and handicaps of individuals with ASD, such as a detailed perception at the expense of a poorer integration into a big picture and, in rare cases, extraordinary performances in tasks such as the numerosity skill or calendar computation, typical of many autistic savants (Dakin & Frith, 2005; Mottron, Dawson, Soulieres, Hubert, & Burack, 2006; Thioux, Stark, Klaiman, & Schultz, 2006). If these speculations were true, ASD symptoms, its enhancements and handicaps, could be the symptoms of the lack of a proper workspace system.

A fundamental open aspect of these results is whether the network changes observed in this experiment reveal structural differences, a distinct pattern of thoughts and mental content during free thinking, or both. Network differences are not likely to be explained by changes in arousal since neither the video-image during the experiment nor the EEG traces revealed any indication of sleep transitions (Ogilvie, 2001). However, as in all resting state experiments, participants where free to elicit any kind of thoughts and it is likely that the mental content may vary across both groups. After completion of the experiment, we interviewed a fraction of our control participants and patients about the contents of their thoughts to specifically address whether ASD patients elicited highly stereotyped, arithmetic or recursive thoughts. While our questionnaire was mostly qualitative, results did not reflect any obvious difference between both groups. Of six interviewed patients the responses were widely varied without specific references to stereotyped thoughts or to a consistent pattern of mental content. One patient (a programmer) reported thoughts about his work, related to the development of an operating system and correspondences with a colleague in Europe. Another thought about the life and events of a famous Argentinean actress and rehearsed several scenes of her acting career. One patient reported thoughts (with imagery) about his pet in different situations, another mentioned that his thoughts were focused on not moving to conform the experimentalist requests and one patient could barely reconstruct his thoughts and reported a very confusing story with lots of pronouns and unspecific pointers (i.e. I thought about things, that changed,…). It is important to remark that while the patients in this study had normal IQs none of them presented savant characteristics. These observations do not demonstrate that changes in the functional network are unrelated to group differences in the patterns of thought. They simply

15

reflect that, if these differences exist, they are not so evident as to be capture by a brief description of mental content. Since the pioneering work of Wundt, (De Groot, 1966; Wundt, 1896) it has become clear that despite obvious systematic difficulties, a detailed quantitative exploration of the content of mental states in relation to the network properties observed during free thought should open a new venue to understand the ultimate goal of cognition, the neural basis of thoughts.

References

Alexander, A. L., Lee, J. E., Lazar, M., Boudos, R., DuBray, M. B., Oakes, T. R., et al. (2007). Diffusion tensor imaging of the corpus callosum in Autism. *Neuroimage, 34*(1), 61-73.

APA. (2000). *Diagnostic and Statistical Manual of Mental Disorders, Fourth Edition, Text Revision*. Washinton DC: American Psychiatric Association.

Baars, B. (1988). *A cognitive theory of consciousness*. New York: Cambridge University Press.

Baars, B. J. (2005). Global workspace theory of consciousness: toward a cognitive neuroscience of human experience. *Prog Brain Res, 150*, 45-53.

Barabasi, A. L. (2009). Scale-free networks: a decade and beyond. *Science, 325*(5939), 412-413.

Batagelj, V., & Mrvar, A. (1998). Pajek – Program for Large Network Analysis. *Connections, 2*, 47-57.

Belmonte, M. K., Allen, G., Beckel-Mitchener, A., Boulanger, L. M., Carper, R. A., & Webb, S. J. (2004). Autism and abnormal development of brain connectivity. *J Neurosci, 24*(42), 9228-9231.

16

Bressler, S. L. (1995). Large-scale cortical networks and cognition. *Brain Res Brain Res Rev, 20*(3), 288-304.

Brown, C., Gruber, T., Boucher, J., Rippon, G., & Brock, J. (2005). Gamma abnormalities during perception of illusory figures in autism. *Cortex, 41*(3), 364-376.

Casanova, M., & Trippe, J. (2009). Radial cytoarchitecture and patterns of cortical connectivity in autism. *Philos Trans R Soc Lond B Biol Sci, 364*(1522), 1433-1436.

Casanova, M. F. v. K., I.A.J, Switala, A. E. van Engeland, H. Heinsen, H, Steinbusch, H.W.M, Hof, P. R. Trippe, J, Stone, J Schmitz, C. (2006). Minicolumnar abnormalities in autism. *Acta Neuropathologica, 112*, 287–303.

Cherkassky, V. L., Kana, R.K , Keller, T.A, Just, M. A. (2006). Functional connectivity in a baseline resting-state network in autism. *Neuroreport, 17*(6), 1687-1690.

Coben, R., Clarke, A. R., Hudspeth, W., & Barry, R. J. (2008). EEG power and coherence in autistic spectrum disorder. *Clin Neurophysiol, 119*(5), 1002-1009.

Courchesne, E., & Pierce, K. (2005). Why the frontal cortex in autism might be talking only to itself: local over-connectivity but long-distance disconnection. *Curr Opin Neurobiol, 15*(2), 225-230.

Dakin, S., & Frith, U. (2005). Vagaries of visual perception in autism. *Neuron, 48*(3), 497-507.

De Groot, A. D. (1966). Perception and memory versus thought: Some old ideas and recent findings. In B. Kleinmuntz (Ed.), *Problem Solving*. New York: Wiley.

Dehaene, S., & Naccache, L. (2001). Towards a cognitive neuroscience of consciousness: basic evidence and a workspace framework. *Cognition, 79*(1-2), 1-37.

Delorme, A., & Makeig, S. (2004). EEGLAB: an open source toolbox for analysis of single-trial EEG dynamics including independent component analysis. *J Neurosci Methods, 134*(1), 9-21.

Di Martino, A., Shehzad, Z., Kelly, C., Roy, A. K., Gee, D. G., Uddin, L. Q., et al. (2009). Relationship between cingulo-insular functional connectivity and autistic traits in neurotypical adults. *Am J Psychiatry, 166*(8), 891-899.

Efron, B., & Tibshirani, R. J. (1994). *An Introduction to the Bootstrap*. New York: Chapman and Hall.

Egaas, B., Courchesne, E., & Saitoh, O. (1995). Reduced size of corpus callosum in

17

autism. *Arch Neurol, 52*(8), 794-801.

Friston, K. (2002). Beyond phrenology: what can neuroimaging tell us about distributed circuitry? *Annu Rev Neurosci, 25*, 221-250.

Frith, U. (1989). *Autism: explaining the enigma*. Oxford, U.K.: Basil Blackwell.

Gallos, L. K., Song, C., Havlin, S., & Makse, H. A. (2007). Scaling theory of transport in complex biological networks. *Proc Natl Acad Sci U S A, 104*(19), 7746-7751.

Galvao, V., Miranda, J. G., Andrade, R. F., Andrade, J. S., Jr., Gallos, L. K., & Makse, H. A. (2010). Modularity map of the network of human cell differentiation. *Proc Natl Acad Sci U S A, 107*(13), 5750-5755.

Gusnard, D. A., & Raichle, M. E. (2001). Searching for a baseline: functional imaging and the resting human brain. *Nat Rev Neurosci, 2*(10), 685-694.

He, B. J., & Raichle, M. E. (2009). The fMRI signal, slow cortical potential and consciousness. *Trends Cogn Sci, 13*(7), 302-309.

He, B. J., Zempel, J. M., Snyder, A. Z., & Raichle, M. E. (2010). The temporal structures and functional significance of scale-free brain activity. *Neuron, 66*(3), 353-369.

Hughes, J. R. (2007). Autism: The first firm finding = underconnectivity? *Epilepsy and Behavior, 11*, 20-24.

Just, M. A., Cherkassky, V. L., Keller, T. A., Kana, R. K., & Minshew, N. J. (2007). Functional and Anatomical Cortical Underconnectivity in Autism: Evidence from an fMRI Study of an Executive Function Task and Corpus Callosum Morphometry. *Cerebral Cortex, 17*, 951--961.

Just, M. A., Cherkassky, V. L., Keller, T. A., & Minshew, N. J. (2004). Cortical activation and synchronization during sentence comprehension in high-functioning autism: evidence of underconnectivity. *Brain, 127*(Pt 8), 1811-1821.

Kamada, T., & Kawai, S. (1989). An algorithm for drawing general undirected graphs. *Information Processing Letters, 31*, 7-15.

Kana, R. K., Keller, T.A. Cherkassky, V. L. Minshew, N.J., Just, M. A. (2006). Sentence comprehension in autism: thinking in pictures with decreased functional connectivity. *Brain, 129*(9), 484-2493.

Kennedy, D. P., Redcay, E., & Courchesne, E. (2006). Failing to deactivate: resting functional abnormalities in autism. *Proc Natl Acad Sci U S A, 103*(21), 8275-8280.

Kleinhans, N. M., Richards, T., Sterling, L., Stegbauer, K. C., Mahurin, R., Johnson, L.

18

C., et al. (2008). Abnormal functional connectivity in autism spectrum disorders during face processing. *Brain, 131*(Pt 4), 1000-1012.

Koshino, H., Carpenter, P. A., Minshew, N. J., Cherkassky, V. L., Keller, T. A., & Just, M. A. (2005). Functional connectivity in an fMRI working memory task in high-functioning autism. *Neuroimage, 24*(3), 810-821.

Latora, V., & Marchiori, M. (2001). Efficient behavior of small-world networks. *Phys Rev Lett, 87*(19), 198701.

Lord, C., Risi, S., Lambrecht, L., Cook, E. H., Jr., Leventhal, B. L., DiLavore, P. C., et al. (2000). The autism diagnostic observation schedule-generic: a standard measure of social and communication deficits associated with the spectrum of autism. *J Autism Dev Disord, 30*(3), 205-223.

Lu, H., Zuo, Y. Gu, H., Waltz, J. A. Zhan, W. Scholl, C.A. Rea, W. Yang. (2007). Synchronized delta oscillations correlate with the resting-state functional MRI signal. *Proceeedings of the National Academy of Sciences, 104*(46), 18265–18269

Markram, H., Rinaldi, T., & Markram, K. (2007). The intense world syndrome--an alternative hypothesis for autism. *Front Neurosci, 1*(1), 77-96.

Mason, R. A., Williams, D. L., Kana, R. K., Minshew, N., & Just, M. A. (2008). Theory of Mind disruption and recruitment of the right hemisphere during narrative comprehension in autism. *Neuropsychologia, 46*(1), 269-280.

McAlonan, G. M., Cheung, V., Cheung, C., Suckling, J., Lam, G. Y., Tai, K. S., et al. (2005). Mapping the brain in autism. A voxel-based MRI study of volumetric differences and intercorrelations in autism. *Brain, 128*(Pt 2), 268-276.

Montez, T., Linkenkaer-Hansen, K., van Dijk, B. W., & Stam, C. J. (2006). Synchronization likelihood with explicit time-frequency priors. *Neuroimage, 33*(4), 1117-1125.

Mottron, L., Dawson, M., Soulieres, I., Hubert, B., & Burack, J. (2006). Enhanced perceptual functioning in autism: an update, and eight principles of autistic perception. *J Autism Dev Disord, 36*(1), 27-43.

Murias, M., Webb, S. J., Greenson, J, Dawson, G. (2008). Resting state cortical connectivity reflected in EEG coherence in individuals with autism. *Biological Psychiatry, 62*(3), 270–273.

Nicoll, A., Larkman, A., & Blakemore, C. (1993). Modulation of EPSP shape and efficacy by intrinsic membrane conductances in rat neocortical pyramidal

neurons in vitro. *J Physiol, 468*, 693-710.

Ogilvie, R. D. (2001). The process of falling asleep. *Sleep Med Rev, 5*(3), 247-270.

Pashler, H., & O'Brien, S. (1993). Dual-task interference and the cerebral hemispheres. *J Exp Psychol Hum Percept Perform, 19*(2), 315-330.

Raichle, M. E. (2009). A paradigm shift in functional brain imaging. *J Neurosci, 29*(41), 12729-12734.

Rubinov, M., & Sporns, O. (2009). Complex network measures of brain connectivity: Uses and interpretations. *Neuroimage*.

Schroeder, C. E., & Lakatos, P. (2009). Low-frequency neuronal oscillations as instruments of sensory selection. *Trends Neurosci, 32*(1), 9-18.

Sergent, C., Baillet, S., & Dehaene, S. (2005). Timing of the brain events underlying access to consciousness during the attentional blink. *Nat Neurosci, 8*(10), 1391-1400.

Sigman, M., & Cecchi, G. A. (2002). Global organization of the Wordnet lexicon. *Proc Natl Acad Sci U S A, 99*(3), 1742-1747.

Sigman, M., & Dehaene, S. (2008). Brain mechanisms of serial and parallel processing during dual-task performance. *J Neurosci, 28*(30), 7585-7598.

Sporns, O., & Zwi, J. D. (2004). The small world of the cerebral cortex. *Neuroinformatics, 2*(2), 145-162.

Stam, C. J., Jones, B. F., Nolte, G., Breakspear, M., & Scheltens, P. (2007). Small-world networks and functional connectivity in Alzheimer's disease. *Cereb Cortex, 17*(1), 92-99.

Thioux, M., Stark, D. E., Klaiman, C., & Schultz, R. T. (2006). The day of the week when you were born in 700 ms: calendar computation in an Autistic savant. *J Exp Psychol Hum Percept Perform, 32*(5), 1155-1168.

Watts, D. J., & Strogatz, S. H. (1998). Collective dynamics of 'small-world' networks. *Nature, 393*(6684), 440-442.

Welchew, D. E., Ashwin, C., Berkouk, K., Salvador, R., Suckling, J., Baron-Cohen, S., et al. (2005). Functional disconnectivity of the medial temporal lobe in Asperger's syndrome. *Biol Psychiatry, 57*(9), 991-998.

Weng, S. J., Wiggins, J. L Peltier S. J Carrasco, M Risi, S, Lord, C Monk, C.S. (2010). Alterations of resting state functional connectivity in the default network in adolescents with autism spectrum disorders. *Brain Research, 1313*, 202-214.

Wicker, B., Fonlupt, P.,Hubert, B., Tardif, C., Gepner, B., Deruelle, C. (2008).

Abnormal cerebral effective connectivity during explicit emotional processing in adults with autism spectrum disorder. *Social Cognitive and Affective Neuroscience, 3*(2), 135-143.

Wundt, W. (1896). *Outline of psychology*. Leipzig: Engelmann

Zylberberg, A., Fernandez Slezak, D., Roelfsema, P. R., Dehaene, S., & Sigman, M. The brain's router: a cortical network model of serial processing in the primate brain. *PLoS Comput Biol, 6*(4), e1000765.

Figure and Table captions

Table 1. Details of ASD subjects: age, diagnosis, IQ and ADOS scores.

Figure 1. Differences in connectivity between ASD and Control groups. a) SL-matrix, averaged for all participants in this study. b) t-values of the SL difference between ASD and controls for each pair of channels. A red (blue) colour in the matrix indicates that SL is increased (decreased) in control compared to ASD population. c) Proportion of links in the SL-matrix remaining after appliance of different SL-value filters. The red line shows the threshold chosen for the analysis. d) Distribution of t-values. Red lines indicate the thresholds chosen for the analysis. e) Binary matrix showing links exceeding the SL threshold. f) Resulting matrix of thresholding the t-value matrix of fig 1b. Values are 1, 0 or -1. g) Combination of both filters gives the matrix valued in 1 and -1 for those links surpassing both filters. h) Topography of the links exceeding the threshold: Blue lines show connections significantly higher in controls, red lines show connections significantly higher in ASD.

Figure 2. SL averaged across different regions. a) Scheme of the four regions defined for this analysis. b) SL connections for all pair or regions (connections are symmetric son only the upper-diagonal triangular matrix is shown). Comparison within the diagonal show within region connections. Local connections in mid frontal and long connections between mid frontal and occipital are diminished in ASD compared to controls. Local connections in both Lateral Frontal areas are enhanced in ASD.

Figure 3. Relation between SL and ADOS. a) Representative links showing a positive and a negative relation between SL and ADOS. b) Topographic projection of the coefficients of the regression, at two different thresholds. Blue lines show negative coefficients (negative relation between SL and ASD severity) and red lines show positive coefficients (positive relation between SL and ASD severity) c) Histograms of coefficients as a function of distance between electrodes. The fraction of positive coefficients decays monotonically as the distance increases. Negative coefficients distribution is more homogeneous and remains significant at longer distances. d) Mean value of correlation coefficients as a function of distance. For short distances, correlations are on average positive, indicating that short range connections increase with ADOS. At long distances, correlations are on average negative indicating that long range connections decrease with ADOS

Figure 4. Relation between IQ, ADOS and SL. a) Scatter plot of the ADOS and IQ scores per ASD subject. b) Beta coefficients for ADOS, from a multiple regression of SL (one for each pair of channels), with IQ and ADOS as regressors. c) Topographic projection of the beta coefficients for ADOS, at threshold =0.05. Blue lines show negative coefficients (negative relation between SL and ASD severity) and red lines show positive coefficients (positive relation between SL and ASD severity) c) Beta coefficients for IQ, from the same multiple regression of SL, with IQ and ADOS as regressors. d) Topographic projection of the beta coefficients for IQ, at threshold =0.05.

Figure 5. Topology of ASD and control functional connectivity networks: a) minimal energy plots of the average networks for both groups. Colors represent the four electrode groups defined in figure 2. b) Average degree as a function of threshold. Control group shows higher degree than ASD. b) Topographic map of the degree at threshold = 0.056. Green dots indicate electrodes where $K_{control} > K_{ASD}$. Pink dots indicate electrodes where $K_{ASD} > K_{control}$, P<0.01) d) Characteristic path length (L) as a function of threshold. Control group shows lower L than ASD. e) Clustering Coefficient (C) as a function of threshold. Control group shows higher C than ASD. f) Modularity as a function of threshold. ASD group shows higher modularity than Controls.

Supplementary Figure 1. Pairs of electrodes displaying differences in connectivity between ASD and control groups at several thresholds.. Blue lines: connections weaker

in ASD than in controls. Red lines: connections stronger in ASD than in controls. a) Different values for the filter of T values (SL-value =0.03). b) Different values for the filter of SL-value (t-value =2).

Supplementary Figure 2. Visualization of ASD and control networks for a fixed threshold of 0.05. The topography of the networks is qualitatively equal to the topography when the degree is fixed.
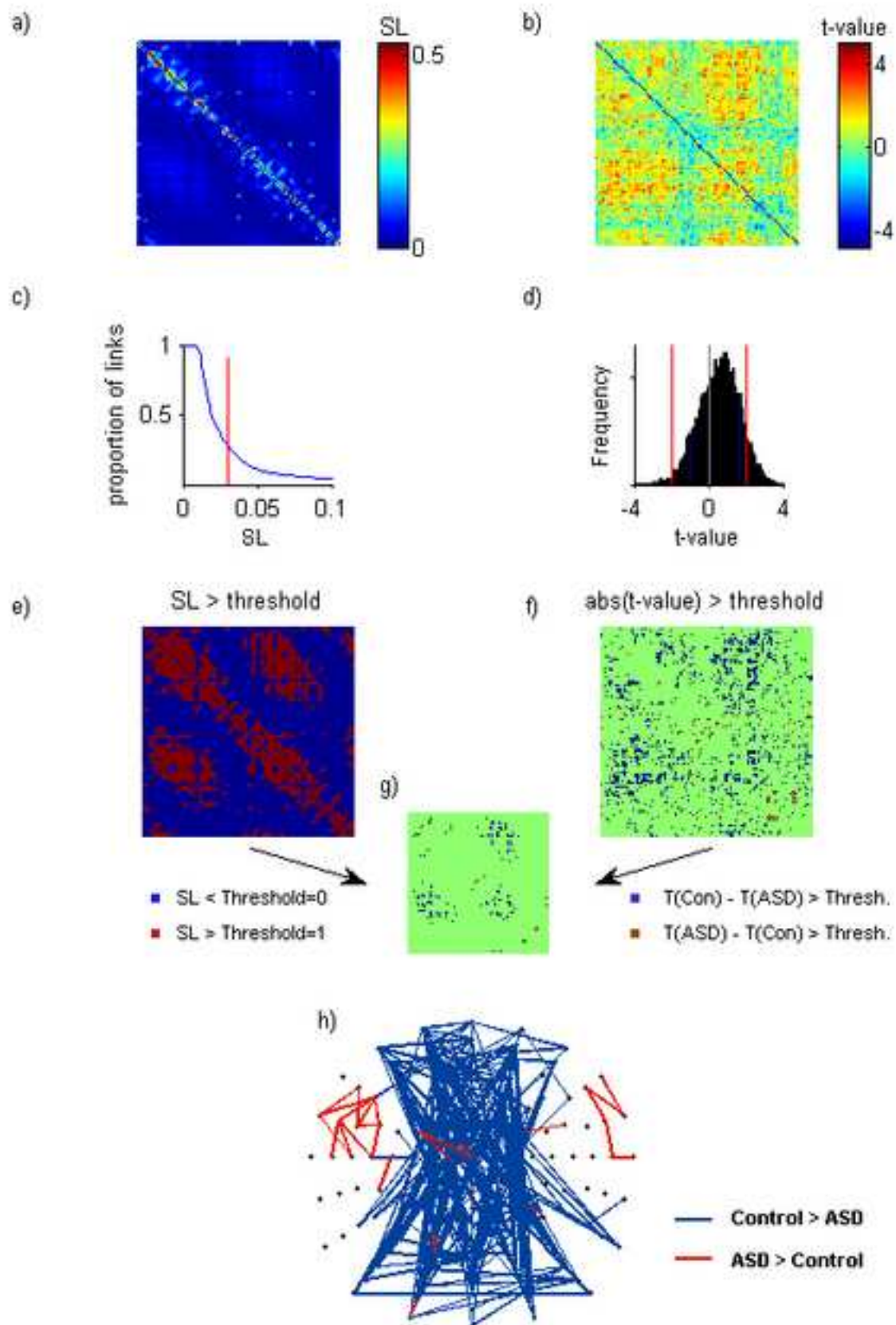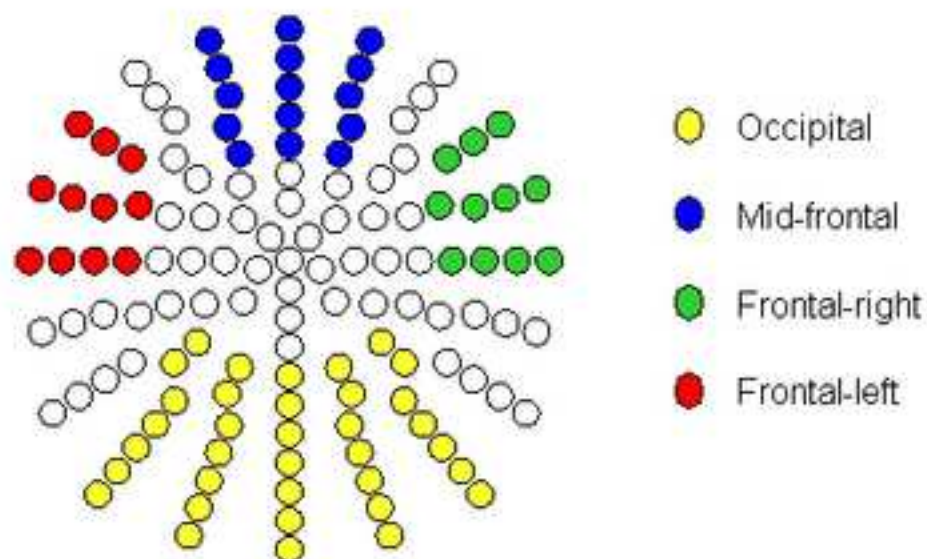
23

research highlights

- Connectivity of EEG delta band is different in ASD and control subjects.

- ASD subjects showed diminished long-range connections, and enhanced short-range connections.

- This altered connectivity pattern is a good predictors of ASD severity.

- ASD networks are more parallel and have less small-world behaviour.
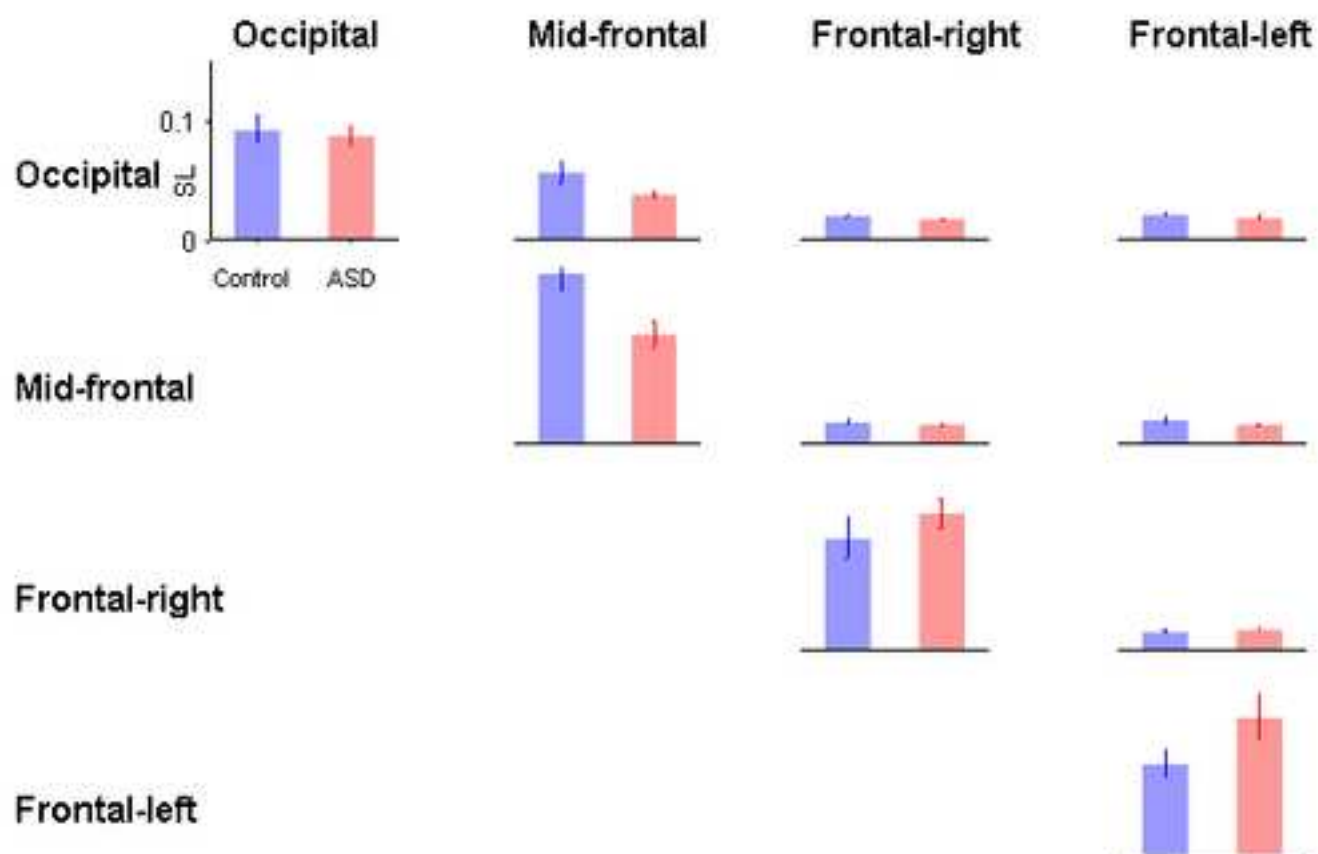
24

Table 1

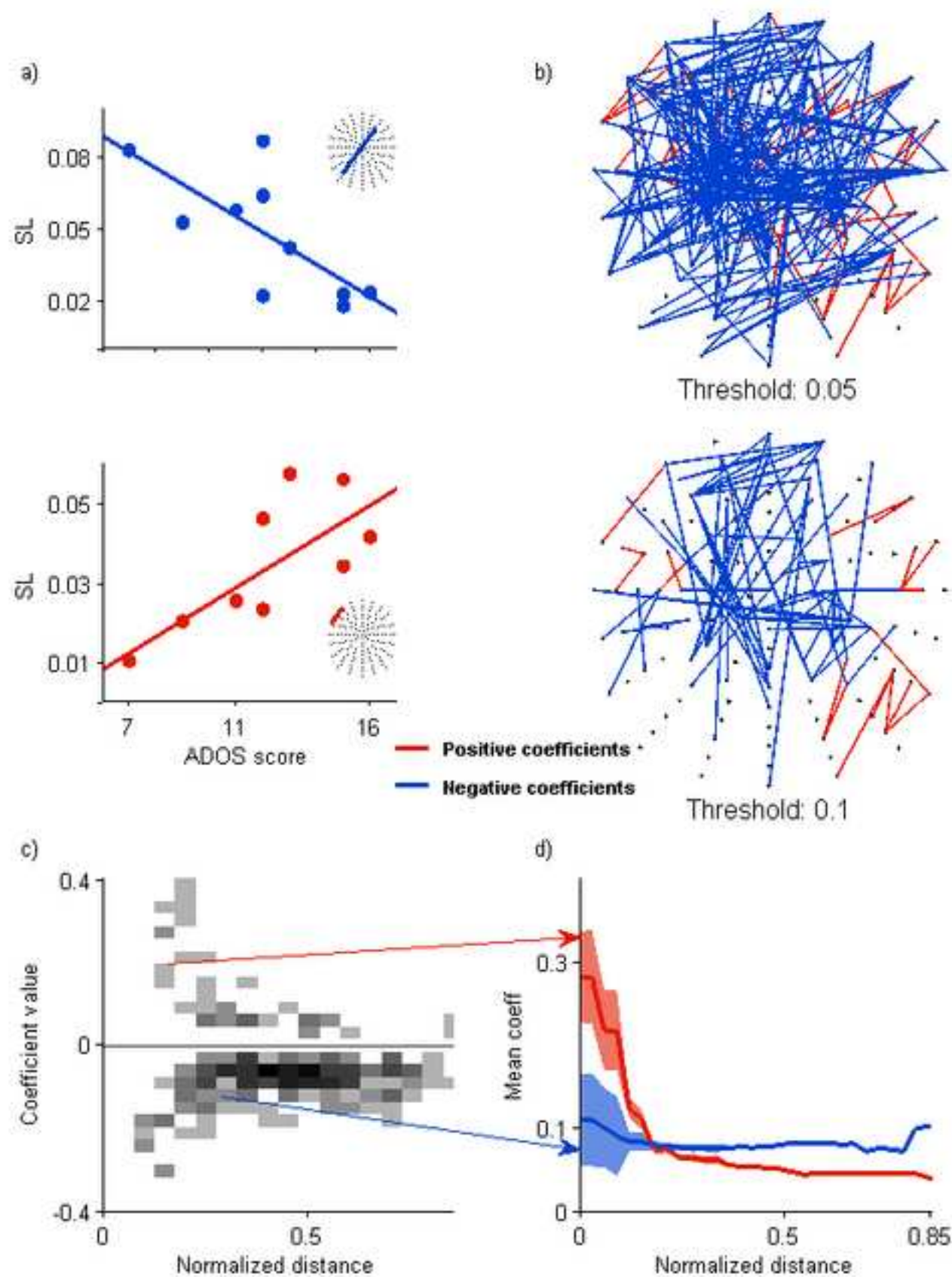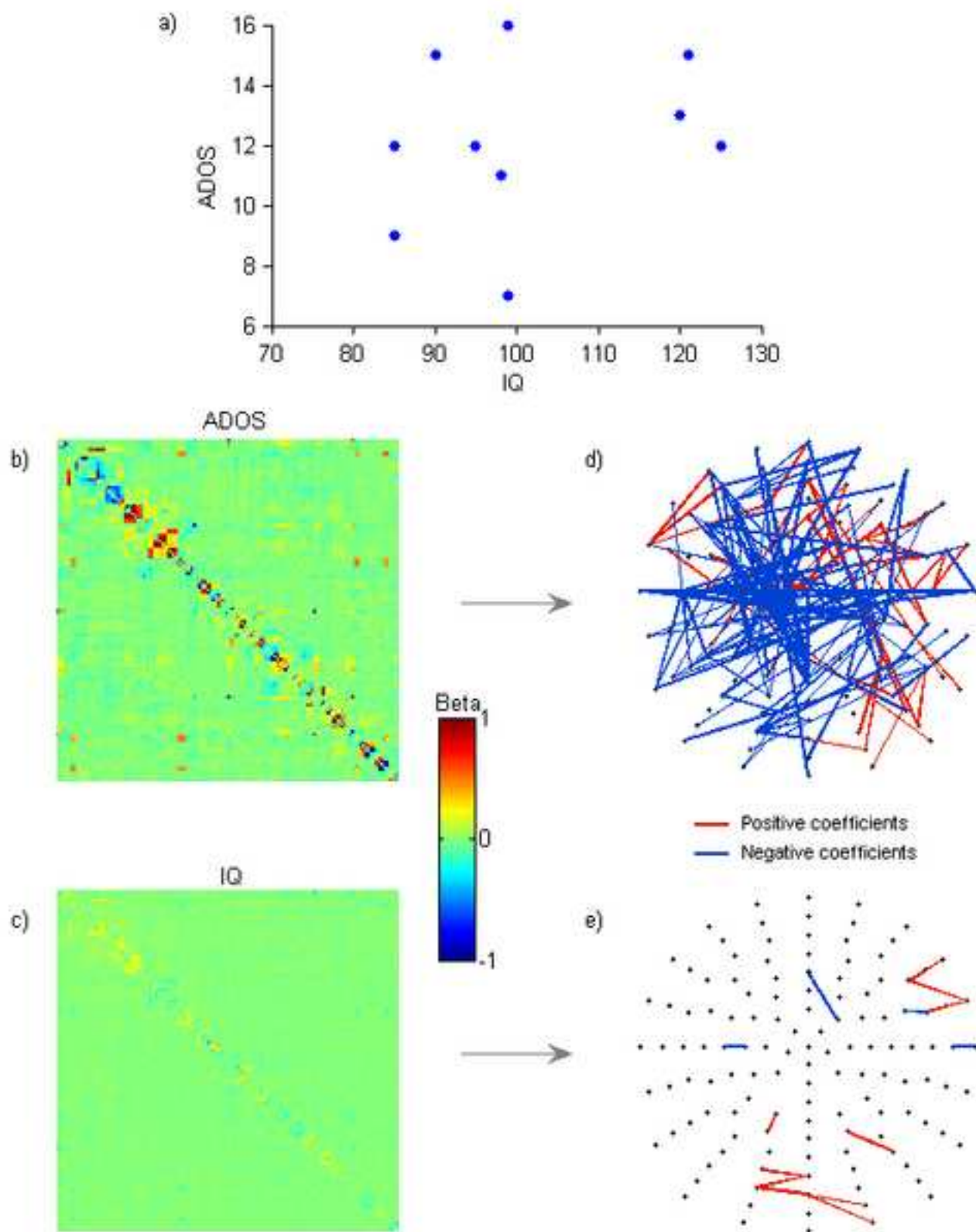| Age	Sex	Diagnosis	Verbal IQ	Exec IQ	Total IQ	ADOS		
						Comm.	Soc. Int.	Total
32	F	Asperger	116	78	99	3	4	7
26	M	HFA	98	80	90	10	5	15
22	M	HFA	96	74	85	3	9	12
17	M	HFA	111	127	120	5	8	13
17	M	Asperger	88	83	85	2	7	9
30	M	HFA	114	130	125	4	8	12
38	M	HFA	111	131	121	6	9	15
24	M	HFA	104	89	98	5	6	11
16	M	HFA	99	89	95	3	9	12
16	M	HFA	94	105	99	6	10	16

Figure 1

Figure 2
ACCEPTED MANUSCRIPT

Figure 3 ACCEPTED MANUSCRIPT

a)

b) Threshold: 0.05

Threshold: 0.1

Positive coefficients
Negative coefficients

c)

d)

Figure 4
ACCEPTED MANUSCRIPT

Figure 5